Title
The simplified thermal modeling approach used in CalME

Authors
Lea, Jeremy D
Harvey, John T

Publication Date
2012

Peer reviewed

THE SIMPLIFIED THERMAL MODELING APPROACH USED IN *CALME*

Jeremy D. Lea
University of California Pavement Research Center
University of California, Davis
Department of Civil Engineering
One Shields Ave
Davis, CA 95616
Tel: +1 (530) 752-4916
jdlea@ucdavis.edu

John T. Harvey
University of California Pavement Research Center
University of California, Davis
Department of Civil Engineering
One Shields Ave
Davis, CA 95616
Tel: +1 (530) 574-6409
jtharvey@ucdavis.edu

Submission Date: 1 August 2011
Words: 4325
Figures: 4
Tables: 4
Total Word Count: 6325

ABSTRACT

This paper details the development of a new 1-D combined finite difference and finite element procedure for calculating in-depth pavement temperatures, which has been implemented in the *CalME* design method. The model is driven by a database of known surface temperatures rather than raw climatic inputs and an energy balance at the surface, since it was noted that the pavement structure had little impact on the surface temperature (if the surface properties remain constant). The model runs quickly, enabling direct simulation of in-depth temperatures while performing Monte Carlo based simulation of pavement reliability. The disadvantages to this approach are that it requires the surface temperatures to be developed independently and that it does not have a coupled moisture model for the prediction of freeze/thaw conditions. The paper also details some anomalies in the output of the Enhance Integrated Climatic Model (used in the new AASHTO mechanistic-empirical design method), that were found during development. Finally, the paper collects various published values for thermal properties of pavement materials, to aid in the implementation of thermal models.

INTRODUCTION

In the development of *CalME*, the future flexible pavement design methodology for the California Department of Transportation, the decision was taken to follow the new AASHTO Mechanistic-Empirical (ME) design method as closely as possible. The AASHTO design method, referred to here as the MEPDG (1), makes use of the Enhanced Integrated Climatic Model (EICM) software (2) to perform calculations of temperature and moisture conditions within the pavement. However, the slow speed of this software is one of the primary reasons for the MEPDG software requiring too much time per run to make Monte Carlo simulation of variability a feasible alternative for calculating reliability (3).

For this reason, an alternative approach to thermal modeling was sought for *CalME*. An initial attempt was to divide California into six climate zones (which has since been increased to nine), and run 30 years of EICM runs on a series of pavements to develop a database of pavement temperatures which could be used to interpolate pavement temperatures at various times and depths within the structure (4). However, the generated database was around 40 GB, which, despite advances in computer storage and internet speeds, is still too large to distribute with the software. Primarily because of the size of the database, further development was required, although as work progressed other reasons for moving from this database arose. It became clear that the interpolation scheme was not always suitable for the wide variety of pavements that could conceivably be designed in *CalME* and that the output data from EICM contained some anomalies that needed to be avoided.

As a result, a new thermal model was developed which could predict temperatures at any depth in the pavement, based only on the surface temperature with time and the temperature at depth, which is assumed constant. This considerably reduced the data storage requirements (to around 100 MB), and allowed calculation to proceed regardless of the pavement structure. The procedure is very fast, requiring less than a second to compute 30 years worth of hourly temperatures. The disadvantages of this approach are that it does not handle moisture changes in the pavement directly (especially freeze/thaw) and requires a pre-computed set of surface temperatures.

This paper details the implementation of this model and the mathematical background, along with the various thermal properties needed as inputs to the model. To begin though, it provides some more details of the issues mentioned above.

BACKGROUND

In modeling the temperature and moisture conditions in pavements, the EICM is generally used, in conjunction with the Climatic Database for Integrated Model (CDIM) software, which downloads weather station information. EICM is now embedded in the MEPDG software (which has been superseded by the recently released Darwin-ME). It is not clear how the MEPDG version differs from the last standalone release of EICM (version 3.0, release January 2003), since it is not possible to run it independently. All of the comments within this document refer to the 3.0 version.

As mentioned in the introduction, the slow speed of the EICM software is one of the primary reasons for the MEPDG not being able to perform Monte Carlo simulation for reliability analysis in a reasonable time. Since improved reliability analysis was a requirement for the *CalME* design method, an alternative to running EICM was sought. The first stage in this process was the development of climate zones for California, choosing representative weather stations for these zones, and running 30 years of historical weather station data in EICM, on a range of pavements, to understand the impact of climate on the pavement. These developments are outlined in (4). The original plan was to distribute the database developed in that project with *CalME* and use an interpolation scheme to predict pavement temperatures, which are required for the prediction of asphalt moduli. However, this would

have required distribution on 10 DVDs, or a 40 GB download, and even today asking people to store this amount of data can be problematic[1].

The initial idea for reducing this data was to develop statistical models for either generating a realistic series of temperatures using a time series model, or to develop models for predicting in depth temperatures based on recent air temperatures—similar to Bell's equation used in FWD back-calculation (5). Only flexible pavements were considered in this modeling, because *CalME* only deals with flexible pavements. While plotting the data in various ways to aid in the development of these statistical models a few things were noticed. The most important was that for each weather station and pavement surface absorptivity and emissivity, the surface temperatures were almost identical.

The differences that were observed in surface temperatures were originally thought to be due to a 'heat reservoir' effect from thicker asphalt pavements. However, this did not match with the pavements that exhibited differences. Further investigation revealed a number of inconsistencies in the data. In (4) 28 different AC pavements were used, generated by a combination of four different granular layers and seven asphalt thicknesses, all on subgrade to a total thickness of 3657.6 mm (144 in). These are labeled AC-2-6-6, etc., in the original report and in this paper, and shown in Table 1. However, the material properties used for the AB and ASB are identical (the EICM defaults for an A-1-a material) and so the AC-X-6-12 and AC-X-12-6 pavements are theoretically identical, although the numerical models are different. Each layer is broken into four elements in the finite difference solution scheme used by EICM, so in the first case the pavement has four 38.1 mm (1.5 in) elements followed by four 76.2 mm (3 in) elements, while in the second case there are four 76.2 mm (3 in) elements, followed by four 38.1 mm (1.5 in) elements. Thus, if the solution scheme is numerically stable and accurate, the results from these pavements should not differ considerably.

TABLE 1 Structures used in development of EICM database

AC Thicknesses	50.8 mm (2 in)	101.6 mm (4 in)	203.2 mm (8 in)	304.8 mm (12 in)	406.4 mm (16 in)	558.8 mm (22 in)	711.2 mm (28 in)
AB Thickness	152.4 mm (6 in)		152.4 mm (6 in)		304.8 mm (12 in)		304.8 mm (12 in)
ASB Thickness	152.4 mm (6 in)		304.8 mm (12 in)		152.4 mm (6 in)		304.8 mm (12 in)

The first inconsistency is that while the 50.8 mm (2 in) AC pavements with a 152.4 mm (6 in) base show the highest daily temperature variation, the 50.8 mm (2 in) AC with 304.8 mm (12 in) base pavements show the lowest, with several degrees Celsius difference. This can be seen on Figure 1. While various explanations were postulated, Figure 2 shows that the most likely cause is some type of numerical problem.

On Figure 2, it can be seen that there are 76.2 mm (3 in) areas at the top of each 304.8 mm (12 in) layer and 38.1 mm (1.5 in) areas at the top of each 152.4 mm (6 in) layer where the slope is not continuous. These are equal to the node spacing, implying some discontinuity in the first element of the granular layer. Not as noticeable on this figure is that there is also a discontinuity between the first element of the third layer (the ASB), and the second element of that layer. Since the same material was used for both layers, there should not be any discontinuity in their behavior. This shows that these are problems caused by numerical issues with the EICM solution scheme. These issues were reported to the developers of the MEPDG software (6), although no response has been received to date. It is not possible to tell if these problems exist in the version embedded in the MEPDG software, since the intermediate temperature results cannot be extracted.

[1] The databases have since been optimized and the size reduced to about 8 GB. However, this is still a considerable amount of data.

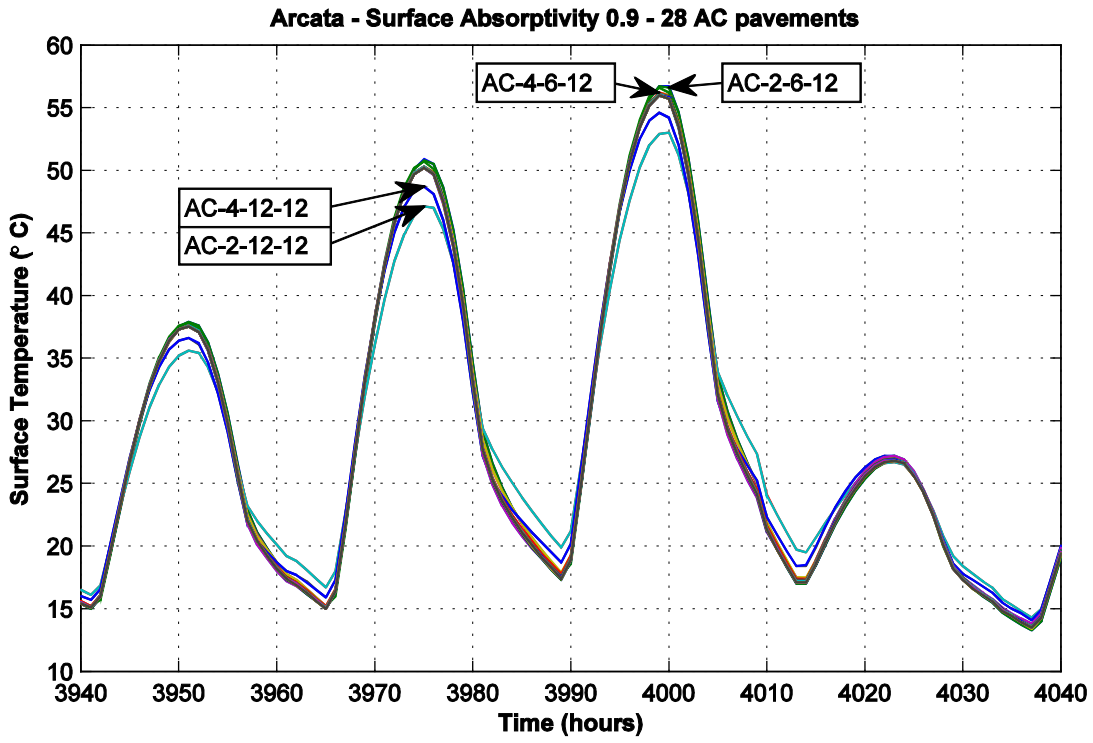

FIGURE 1 Example comparison of surface temperatures across all AC pavements

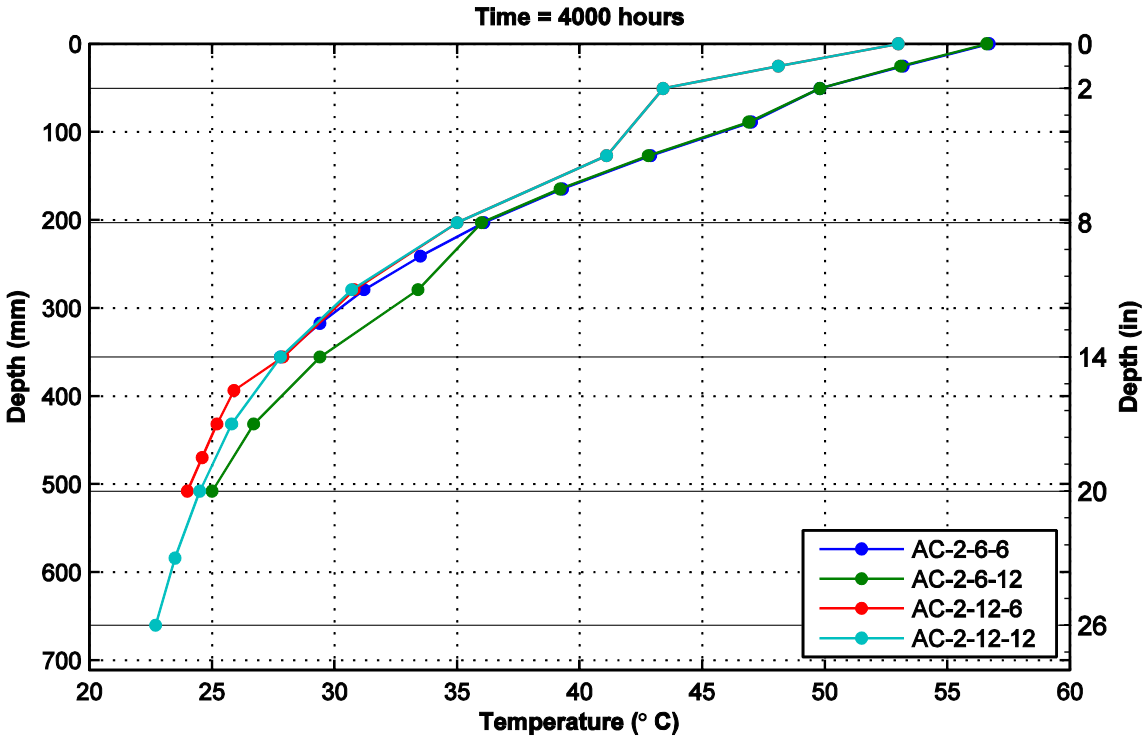

FIGURE 2 Differences in pavement temperatures at one example time

These calculation errors are not very large at most times (<10°C at the extremes), so may not have any impact on MEPDG results, although, based on these findings, it was decided to discontinue development of statistical models of in-depth temperatures, since these anomalies introduced trends

that ran counter to engineering judgment. To account for in-depth temperatures it was thus necessary to model the in-depth temperatures directly based on the principles of thermal conduction (essentially a reimplementation of the thermal model used by EICM, without the coupled moisture model). Since the surface temperatures across all of the pavements were very similar it was decided to use the surface temperatures as the driver for the model, rather than the raw climatic data. This allows the equations to be solved using a 1-D Galerkin Finite Element (FE) formulation with a Finite Difference (FD) time step, rather than requiring a FD solution in both space and time.

MODEL DETAILS

Heat transfer problems, in one spatial dimension, are governed by the following partial differential equation (PDE), which is called Fourier's Law of Conduction:

$$\frac{\partial T}{\partial t} = \alpha \frac{\partial^2 T}{\partial z^2} = \frac{k}{\rho c_p} \frac{\partial^2 T}{\partial z^2} \qquad \text{.....(1)}$$

where:
T = The temperature (K)
t = The time (s)
z = The depth (m)
α = The thermal diffusivity ($m^2 \cdot s^{-1}$)
k = The thermal conductivity ($W \cdot m^{-1} \cdot K^{-1}$)
ρ = The density ($kg \cdot m^{-3}$)
c_p = The specific heat capacity ($J \cdot m^{-3} \cdot K^{-1} = W \cdot s \cdot m^{-3} \cdot K^{-1}$)

This is the so-called 'strong form' of the PDE, which needs to be solved across the domain. A complicated solution to this problem for multi-layered media was recently presented in (7), based on the same theory used for layered elastic analysis of pavements, and which incorporates an axi-symmetric 2-D temperature distribution. Since this solution requires extensive numerical integration, and because the temperatures are constrained to an infinite periodic sequence, it was not considered.

Since the incremental recursive ME design process, pioneered by *CalME*, steps forward in time, it is natural to consider a forward finite difference solution which generates a solution at some time $t+\Delta t$ based on the information available at time t. This fits well with the first order differential with time in Equation (1). EICM, along with most other computer codes that implement a solution to this problem, also uses a FD step for the changes with depth, since the solution for the energy flux through the surface boundary requires a simultaneous solution of the temperature at the surface and the thermal flux at the surface. These types of boundary conditions are not generally compatible with the FE method. However, if the solution is restricted to using the temperature at the surface as a known variable, then the depth component can be solved using the FE method.

Returning to the problem at hand, the first step is to apply a FD solution for the time step. The classic solution is to use Newmark's Beta Method, which uses the following approximations:

$$\left.\frac{\partial T}{\partial t}\right|_{t+\Delta t} \approx \left.\frac{\partial T}{\partial t}\right|_t + \left((1-\gamma) \left.\frac{\partial^2 T}{\partial t^2}\right|_t + \gamma \left.\frac{\partial^2 T}{\partial t^2}\right|_{t+\Delta t} \right) \Delta t$$

$$T_{t+\Delta t} \approx T_t + \left.\frac{\partial T}{\partial t}\right|_t \Delta t + \left(\left(\frac{1}{2} - \beta\right) \left.\frac{\partial^2 T}{\partial t^2}\right|_t + \beta \left.\frac{\partial^2 T}{\partial t^2}\right|_{t+\Delta t} \right) (\Delta t)^2$$

where:
γ, β = Constants
Δt = The time step (s)

It is common to use γ=½ ,β=¼, so the equations simplify to:

$$\left.\frac{\partial T}{\partial t}\right|_{t+\Delta t} \approx \left.\frac{\partial T}{\partial t}\right|_{t} + \left(\left.\frac{\partial^2 T}{\partial t^2}\right|_{t} + \left.\frac{\partial^2 T}{\partial t^2}\right|_{t+\Delta t}\right)\frac{\Delta t}{2}$$

$$T_{t+\Delta t} \approx T_t + \left.\frac{\partial T}{\partial t}\right|_{t}\Delta t + \left(\left.\frac{\partial^2 T}{\partial t^2}\right|_{t} + \left.\frac{\partial^2 T}{\partial t^2}\right|_{t+\Delta t}\right)\left(\frac{\Delta t}{2}\right)^2$$

Both equations contain the second order differential of temperature with respect to time at the new time, which unknown. To solve, combine the equations to eliminate this:

$$\left.\frac{\partial^2 T}{\partial t^2}\right|_{t+\Delta t}\left(\frac{\Delta t}{2}\right)^2 \approx T_{t+\Delta t} - T_t - \left.\frac{\partial T}{\partial t}\right|_{t}\Delta t - \left.\frac{\partial^2 T}{\partial t^2}\right|_{t}\left(\frac{\Delta t}{2}\right)^2$$

$$\left.\frac{\partial T}{\partial t}\right|_{t+\Delta t} \approx \frac{2\left(T_{t+\Delta t} - T_t\right)}{\Delta t} - \left.\frac{\partial T}{\partial t}\right|_{t} \qquad \text{.....(2)}$$

This gives a formula which can then be used to expand Equation (1):

$$\left.\frac{\partial T}{\partial t}\right|_{t+\Delta t} \approx \frac{2\left(T_{t+\Delta t} - T_t\right)}{\Delta t} - \left.\frac{\partial T}{\partial t}\right|_{t} = \alpha\left.\frac{\partial^2 T}{\partial z^2}\right|_{t+\Delta t} \qquad \text{.....(3)}$$

This is now an ordinary differential equation in one variable, *z*, so is now suitable for transformation into a 1-D Galerkin FE formulation over a domain (0,*D*). The temperature at both ends of the domain is assumed to be known (based on the input data) at all time steps. This could also be solved using a thermal flux at the surface rather than the temperature, but this is not expanded here.

The development of the FE component follows a classic 1-D treatment that can be found in any introductory text (e.g. 8). The FE approximation of the domain is formed using *N* nodes, with *N*-1 linear (2-node) elements. The basis functions for each node are given in an element relative coordinate system, for element *e*, with coordinate $\xi_e \in (-1,1)$. These are given by:

$$\phi_1(\xi_e) = \tfrac{1}{2}(1-\xi_e) \quad \phi_2(\xi_e) = \tfrac{1}{2}(1+\xi_e) \quad z(\xi_e) = \sum_{i=1}^{2}\phi_i(\xi_e)\, z_i$$

where: z_i = The nodal depth (*z* coordinate) of the i^{th} elemental node.

These basis functions can also be used to define an element local trial and weighting functions:

$$\hat{T}^e(\xi_e) = \sum_{i=1}^{2}\phi_i(\xi_e)\, T_i^e \quad \hat{w}^e(\xi_e) = \sum_{i=1}^{2}\phi_i(\xi_e)\, w_i^e$$

where: T_i^e = The nodal temperature at node *i* in element *e,*
w_i^e = The weight of node *i* in element *e.*

In addition, a nodal mapping function *I*(*i*,*e*) can be defined that takes the local node number *i* and the global element number *e* and maps these to global node numbers:

$$I(i,e) = e + i - 1$$

This can be used to develop global trial and weighting functions (with the temperatures now explicitly referenced to time *t*):

$$\hat{T}(z)\Big|_t = \sum_{e=1}^{N-1}\sum_{i=1}^{2}\phi_i\left(\xi_e(z)\right)T^t_{I(i,e)} \quad \hat{w}(z) = \sum_{e=1}^{N-1}\sum_{i=1}^{2}\phi_i\left(\xi_e(z)\right)w_{I(i,e)}$$

where: $\xi_e(z)$ = A reverse coordinate mapping for element *e*.

Returning to the Equation (3), we can convert the strong form of the PDE to a weak form based on the weighting function (assuming some non-zero nodal weights):

$$0 = \alpha^e\left.\frac{\partial^2\hat{T}(z)}{\partial z^2}\right|_{t+\Delta t} + \frac{2\left(\hat{T}_t(z)-\hat{T}_{t+\Delta t}(z)\right)}{\Delta t} + \left.\frac{\partial\hat{T}(z)}{\partial t}\right|_t$$

$$0 = \int_0^D\left(\alpha^e\left.\frac{\partial^2\hat{T}(z)}{\partial z^2}\right|_{t+\Delta t} + \frac{2\left(\hat{T}_t(z)-\hat{T}_{t+\Delta t}(z)\right)}{\Delta t} + \left.\frac{\partial\hat{T}(z)}{\partial t}\right|_t\right)\hat{w}(z)dz$$

$$0 = \alpha^{N-1}\left.\frac{\partial\hat{T}}{\partial z}\right|_{\substack{t+\Delta t\\ z=D}}\hat{w}(D) - \alpha^1\left.\frac{\partial\hat{T}}{\partial z}\right|_{\substack{t+\Delta t\\ z=0}}\hat{w}(0) - \int_0^D\left.\frac{\partial\hat{T}(z)}{\partial z}\right|_{t+\Delta t}\alpha^e\frac{\partial\hat{w}(z)}{\partial z}dz$$

$$+\frac{2}{\Delta t}\int_0^D\hat{T}_t(z)\hat{w}(z)dz - \frac{2}{\Delta t}\int_0^D\hat{T}_{t+\Delta t}(z)\hat{w}(z)dz + \int_0^D\left.\frac{\partial\hat{T}(z)}{\partial t}\right|_t\hat{w}(z)dz$$

Notice that the thermal diffusivity α is now allowed to be per element (α^e). Since the choice of weighting function is arbitrary, as long as it is non-zero within the domain, the choice can be limited to functions where w_1=0 and w_N=0, eliminating the first two terms. In addition, expanding the functions, performing some manipulation, and exploiting the fact that the integrals of the element basis functions are only non-zero within the element, allows this to be converted back to an element local formulation:

$$0 = -\sum_{e=1}^{N-1}\sum_{i=1}^{2}\sum_{j=1}^{2}\alpha^e T^{t+\Delta t}_{I(i,e)}\int_{-1}^{1}\frac{\partial\phi_i\left(\xi_e\right)}{\partial\xi_e}\frac{\partial\phi_j\left(\xi_e\right)}{\partial\xi_e}\frac{\partial\xi_e}{\partial z}d\xi_e w_{I(j,e)}$$

$$+\sum_{e=1}^{N-1}\sum_{i=1}^{2}\sum_{j=1}^{2}\left(\frac{2}{\Delta t}\left(T^t_{I(i,e)} - T^{t+\Delta t}_{I(i,e)}\right) + \frac{\partial T^t_{I(i,e)}}{\partial t}\right)\int_{-1}^{1}\phi_i\left(\xi_e\right)\phi_j\left(\xi_e\right)\frac{\partial z}{\partial\xi_e}d\xi_e w_{I(j,e)}$$

From this formulation, and the definitions of the basis functions, it is clear that the integrations can be performed analytically. This avoids the numerical integration common in higher dimensional FE formulations, the associated tracking of behavior at Gauss points, and much of the work of 'stiffness matrix' assembly. Example results for element local integrations (with *i*=1 and *j*=1) are:

$$k^e_{11} = \alpha^e\int_{-1}^{1}\frac{\partial\phi_i\left(\xi_e\right)}{\partial\xi_e}\frac{\partial\phi_j\left(\xi_e\right)}{\partial\xi_e}\frac{d\xi_e}{dz}d\xi_e = \frac{\alpha^e}{z_2 - z_1}$$

$$f^e_{11} = \int_{-1}^{1}\phi_i\left(\xi_e\right)\phi_j\left(\xi_e\right)\frac{dz}{d\xi_e}d\xi_e = \frac{z_2 - z_1}{2}\frac{2}{3}$$

In a matrix form this gives two element local matrices:

$$\mathbf{k}^e = \frac{\alpha^e}{z_2 - z_1}\begin{pmatrix} 1 & -1 \\ -1 & 1 \end{pmatrix} \qquad \mathbf{f}^e = \frac{z_2 - z_1}{2}\begin{pmatrix} \frac{2}{3} & \frac{1}{3} \\ \frac{1}{3} & \frac{2}{3} \end{pmatrix}$$

There are *N* known temperatures and *N* known temperature gradients for the current time *t*, two known temperatures (at node 1 and node *N*) for the next time step $t+\Delta t$, two known weights (zero at nodes 1 and *N*), *N*-2 unknown temperatures for the next time step and *N*-2 arbitrary weights. Setting each weight, in turn, to one while the others are zero results in a set of *N*-2 equations:

$$\left(k_{21}^{I-1} + \frac{2}{\Delta t} f_{21}^{I-1}\right) T_{I-1}^{t+\Delta t} + \left(\left(k_{22}^{I-1} + k_{11}^{I}\right) + \frac{2}{\Delta t}\left(f_{22}^{I-1} + f_{11}^{I}\right)\right) T_I^{t+\Delta t}$$
$$+\left(k_{12}^{I} + \frac{2}{\Delta t} f_{12}^{I}\right) T_{I+1}^{t+\Delta t} = f_{21}^{I-1}\left(\frac{2}{\Delta t} T_{I-1}^{t} + \frac{\partial T_{I-1}^{t}}{\partial t}\right)$$
$$+\left(f_{22}^{I-1} + f_{11}^{I}\right)\left(\frac{2}{\Delta t} T_I^t + \frac{\partial T_I^t}{\partial t}\right) + f_{12}^{I}\left(\frac{2}{\Delta t} T_{I+1}^{t} + \frac{\partial T_{I+1}^{t}}{\partial t}\right) \qquad I = 2..N-1$$

This lends its self to a banded matrix representation, with the introduction of an additional vector **d** defined by:

$$d_I^t = \frac{2}{\Delta t} T_I^t + \frac{\partial T_I^t}{\partial t} \qquad I = 2..N-1 \qquad \text{.....(4)}$$

This system can be restored to a system of *N* equations by including the top and bottom node temperatures, and the symmetry can be restored through the standard technique of zeroing the first and last column of the fully formed 'stiffness matrix.' The final form of the system is[2]:

$$\left(\mathbf{K} + \frac{2}{\Delta t}\mathbf{F}\right)\mathbf{T}^{t+\Delta t} = \mathbf{F}\mathbf{d}^t - \begin{bmatrix} -T_1^{t+\Delta t} \\ \left(\alpha^1 k_{21}^1 + \frac{2}{\Delta t} f_{21}^1\right) T_1^t \\ \vdots \\ 0 \\ \vdots \\ \left(\alpha^{N-1} k_{12}^{N-1} + \frac{2}{\Delta t} f_{12}^{N-1}\right) T_N^t \\ -T_N^{t+\Delta t} \end{bmatrix} \qquad \text{.....(5)}$$

This is a linear system of equations, with a banded positive definite coefficient matrix. This can be solved by any technique, although the Cholesky decomposition is the most efficient. The combined matrix on the left hand side can be decomposed before beginning iterative calculations. The vector of gradients **d** can be updated as follows, based on Equations (2) and (4):

$$\mathbf{d}^{t+\Delta t} = \frac{4}{\Delta t}\mathbf{T}^{t+\Delta t} - \mathbf{d}^t$$

[2] **T** is a column vector and not a matrix, but the upper case letter is retained to avoid confusion of time and temperature.

T is initialized to whatever initial temperature profile is chosen (typically a linear interpolation between the first surface temperature and the fix temperature at depth), and then:

$$\mathbf{d}^0 = \frac{2}{\Delta t}\mathbf{T}^0$$

This provides all of the pieces needed for an incremental solution of the equation. Since this is a 1-D FE solution it is very easy to see how it can be expanded from 2-node linear elements to 3-node quadratic or even higher order elements, although the mathematics becomes a little more complex and requires resorting to a slightly more complex and comprehensive explanation of the Galerkin FE method. Mesh generation is left as an exercise for the reader, since generating meshes in 1-D layered media is not difficult, but depends on the exact problem being solved.

TESTING

The only means available to test this method is using the solution for a homogenous semi-infinite half space. In this case, Equation (1) can be solved exactly, provided the driving temperature at the surface is sinusoidal, and the temperature at infinite depth is constant (and equal to the mean surface temperature). The solution, with two sine waves, one annual and one daily, is:

$$\begin{aligned} T(t,z) = T_a &+ T_y \exp\left(-z / D_y\right)\sin(\omega_y t - z / D_y + \phi_y) \\ &+ T_d \exp\left(-z / D_d\right)\sin(\omega_d t - z / D_d + \phi_d) \end{aligned} \qquad \text{.....(6)}$$

$$D_y = \sqrt{\frac{2\alpha}{\omega_y}} \quad D_d = \sqrt{\frac{2\alpha}{\omega_d}}$$

where: T_a = The average temperature (°C),
T_y, T_d = The yearly and daily temperature fluctuation (°C),
ω_y, ω_d = The yearly and daily frequency (h^{-1}),
ϕ_y, ϕ_d = The yearly and daily phase lag.

Figure 3 shows the error between this equation and the FD/FE solution described above, with T_a=15°C, T_y=10°C, T_d=5°C, and α=2000 $mm^2 \cdot h^{-1}$. The periods are ω_y=1/(365×24 h) and ω_d=1/24 h, and the phase lags are three months and three hours respectively. The solution has 800 elements each 25 mm deep. It is initialized with the true values of temperature and temperature gradient from the equation (6) (which is not possible in general), at time t=0, and at both the top and bottom nodes at all times (rather than fixing the temperature at 20 m). The plot only covers the top 4 m of the pavement, since the temperatures below are almost constant, and the first 10000 hours, since the pattern continues to repeat for the remainder of the 30 years.

As can be seen the maximum error is a little over 0.0015°C, or 0.1%, which is very good for a numerical simulation. Obviously, under normal circumstances, the initial temperature profile and gradient are not known, so there is some lag time until the FE solution matches the exact solution.

Although this model is not attempting to predict actual pavement temperatures based on climatic inputs, the model was tested against a number of temperature series from Heavy Vehicle Simulator (HVS) tests. Figure 4 shows one example, from a short rutting test, where the temperature at 50 mm was to be held at 50°C. The temperature at depth was held constant at 35°C. This pavement has a 120 mm AC surface and 450 mm AB on a clay subgrade. The thermal properties of the materials are the default values used in *CalME*. As can be seen the temperatures match fairly well. Using as-built layer thicknesses, and calculated thermal properties for the materials improves the comparison, although the measured temperatures at depth in this case are slightly over the actual temperature

because the thermo-couples are installed in a hole drilled from the surface, which means that the surface temperature responds more quickly to changes in air temperature than the material.

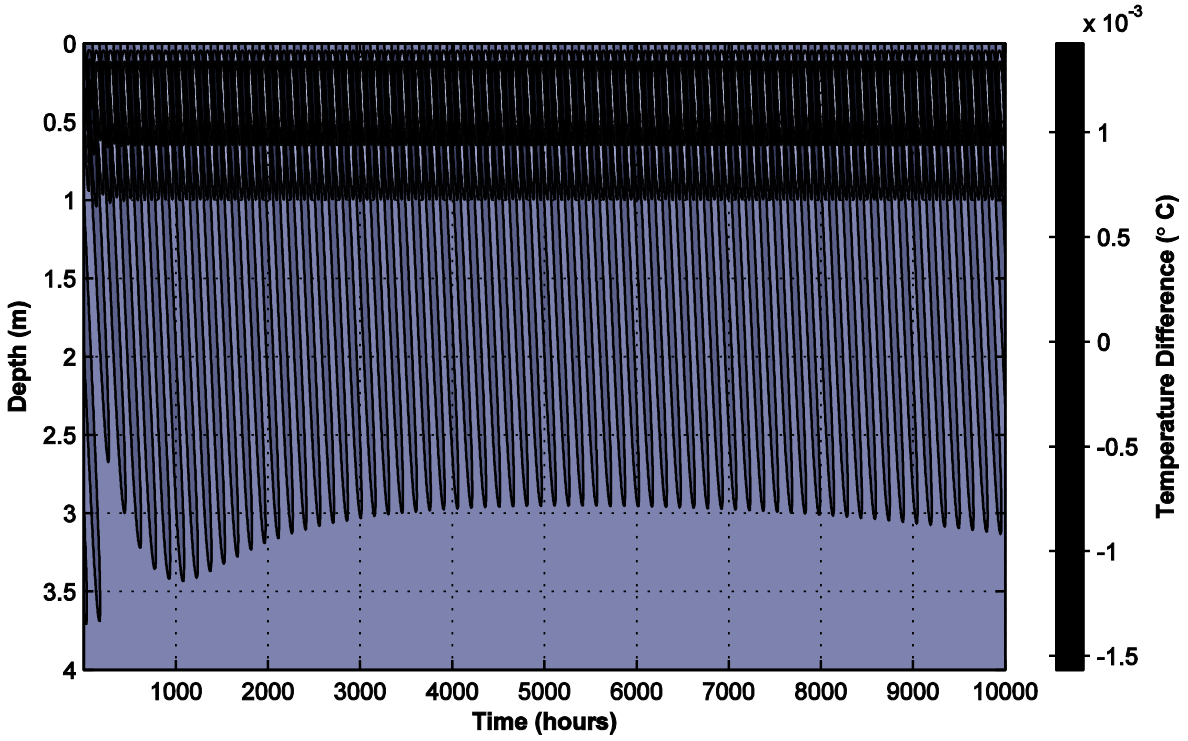

FIGURE 3 Error between exact and finite element solution

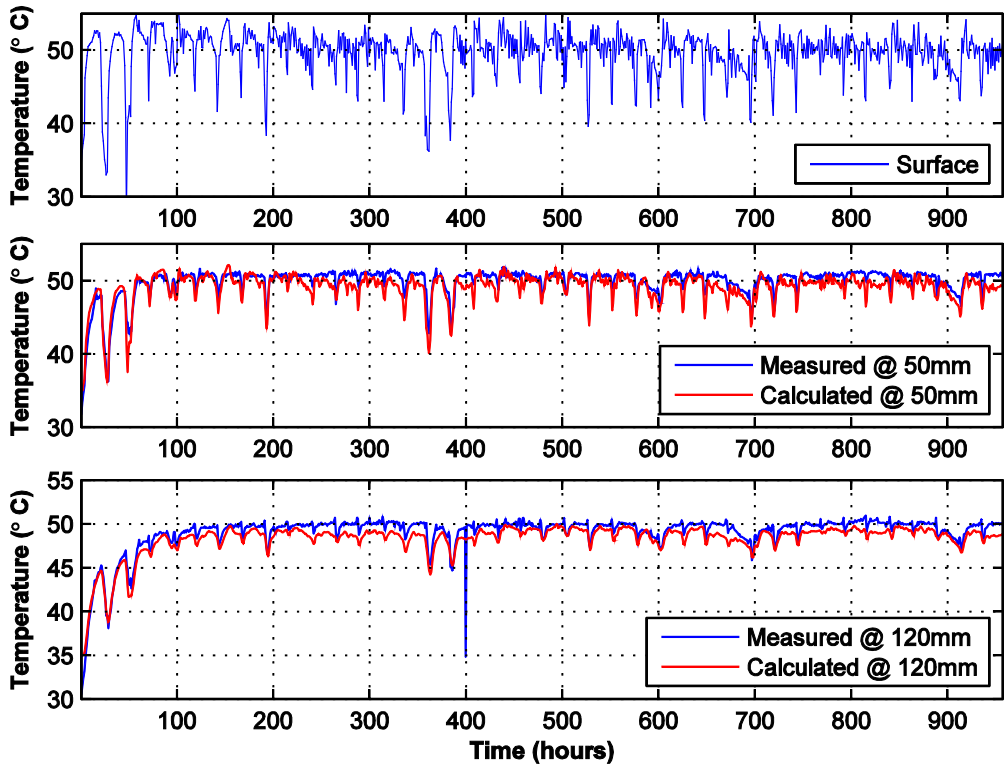

FIGURE 4 Example comparison to measured temperature series.

THERMAL PROPERTIES OF PAVEMENT MATERIALS

The thermal behavior of pavements is largely dependent on the thermal properties of pavement materials, including thermal conductivity, specific heat capacity, density, solar reflectivity/albedo, and thermal emissivity of the surface material. This section provides some examples from literature of these properties, in addition to those provided in the MEPDG.

The following tables provide some recent values for these properties, with Table 2 covering Portland Cement concrete of various types and Table 3 covering Asphalt Concrete. In addition Côté and Konrad (14,15,16) provide data for various base course materials, along with two models for predicting thermal conductivity, and the Fast All-season Soil STrength (FASST) computer program (17), which is similar to EICM, has a simple model for all of USGS soil classifications, along with asphalt and concrete. These last values were adopted for *CalME*, since they were the only complete set of data, and are shown in Table 4.

TABLE 2 Published values for thermal properties for Portland Cement Concrete

Reference	Study	c_p ($Jkg^{-1}K^{-1}$)	k ($Wm^{-1}K^{-1}$)	Material
(10)	Kaloush (2008)	1016	1.719	PCC
		1055		CR PCC (80)[a]
		992		CRPCC (160)[a]
		956		CRPCC (240)[a]
		964		PF PCC (0)[b]
		997		PF PCC (3)[b]
		977		PF PCC (5)[b]
		971		PF PCC (8)[b]

a. Crumb rubber PCC ($lbyd^{-3}$); b. Plastic Fiber modified PCC (% content)

TABLE 3 Published values for thermal properties for Asphalt Concrete (after 13)

Reference	Study	ρ (kgm^{-3})	c_p ($Jkg^{-1}K^{-1}$)	k ($Wm^{-1}K^{-1}$)	α ($m^2s^{-1}\times10^{-6}$)	Material
(11)	Xu and Solaimanian (2010)	2313	880	2.88	.142	AC[a]
			987	0.896		HMA
(10)	Kaloush (2008)		977			GGAC
			875			AR OGFC
(12)	Mrawira and Luca (2006)	2410	1630-2000	1.96-2.01	.41-.53	HMA[b]
		2420	1480-1890	1.91-1.94	.42-.54	HMA[c]
	Luca and Mrawira (2005)	2297-2450	1475-1853	1.623-2.060	.43-.55	AC
	Luca and Mrawira (2002)	2440	766.6	1.75	.936	AC
	Mrawira and Luca (2001)				.407-1.194	AC
	Tan et al. (1997)			1.300-1.420	.536-.580	AC
	Solaimanian and Bolzan (1993)			0.744-2.889		AC
	Himeno et al. (1987)				.600-.110	AC
(13)	Phukan (1985)			1.050-1.520		AC
	Highter and Wall (1984)		800-1600	0.800-1.600	.350-.750	AC
	Johnston (1981)		1674	1.05-1.52		AC
	Wolfe et al. (1980)		879-963	1.003-1.747	.516-.826	AC
	Kavianipour and Beck (1977)			2.280-2.880	.115-.144	AC
	Jordan and Thomas (1976)			0.80-1.42		AC
	Corlew and Dickson (1968)		921	1.210	.587	AC

a. AV 5.8%; b. with gravel, AV 4%; c. w/ Hornfel, AV 4%

TABLE 4 Default thermal diffusivity used in *CalME*

Material	Code	α (mm^2h^{-1})
Portland Cement Concrete	CC	1696
Asphalt Concrete	AC	2000
Bed Rock	BR	3333
Gravel - Well graded	GW	3490
Gravel - Poorly graded	GP	4540
Silty Gravel	GM	3215
Clayey Gravel	GC	3086
Sand - Well graded	SW	3706
Sand - poorly graded	SP	2952
Silty Sand	SM	1963
Clayey Sand	SC	2647
Silt - Low plasticity	ML	1598
Clay - Low plasticity	CL	1360
Organic Clay - Low plasticity	OL	1166
Silt - High plasticity	MH	1472
Clay - High plasticity	CH	1292
Organic Clay - High plasticity	OH	937

CONCLUSIONS

This paper details the development of simplified thermal model used in *CalME*. The model uses pre-calculated surface and at-depth temperatures, and a combination of finite element and finite difference techniques to calculate temperatures within the pavement. The model runs very fast, taking less than a second to compute 30 years of hourly temperatures on modern hardware. As a result, it can be used to calculate temperature profiles for each run in a Monte Carlo simulation of pavement performance. This is one of the main factors in allowing *CalME* to use this technique for reliability analysis. The main disadvantage of this approach is that the method requires a database of surface temperatures, which needs to be stored for each climate region/weather station in use, and for each surface albedo and surface thermal emissivity in use. In *CalME* a limited set of data for California climate regions is provided. However, since one of the primary observations leading to this method was that pavement structure has little impact on pavement surface temperature, a more robust approach would be to use one run of a more complex model, such as EICM, with the deterministic 'mean' pavement design, and use the resulting surface temperatures in later Monte Carlo simulations.

The second drawback of this approach is that it does not use a coupled soil moisture model, which can account for freeze/thaw and other moisture related changes to the thermal properties. More research is needed in this area, but it is expected that using the results from a single run of a more complex model would provide an adequate approximation of the freeze/thaw behavior in a reliability simulation.

Although computational speed was the main motivation for the development of this model, the approach adopted here was chosen because other, possibly faster, approaches were not feasible. In particular, a database of pre-calculated in-depth temperatures was too large for distribution, and still had issues with extrapolation under some innovative designs. Statistical modeling of the temperatures was not pursued after it was found that the in-depth temperatures calculated in the database were flawed. Since the approach detailed above is fast enough for practical use, it is unlikely that statistical modeling will be pursued in the future, since it also suffers from difficulties with extrapolating to unusual pavement designs, and tends to under-predict the true variability in pavement temperatures.

Finally, the paper catalogs some of the newer research into the thermal properties of pavement materials, to expand on the values provided in the EICM/MEPDG documentation.

ACKNOWLEDGEMENTS

This work was undertaken with funding from the California Partnered Pavement Research Program of the California Department of Transportation, Division of Research and Innovation, which is greatly appreciated. The opinions and conclusions expressed in this paper are those of the authors and do not necessarily represent those of Caltrans or the Federal Highway Administration. The assistance of Hui Li in collating the tables of thermal properties is gratefully acknowledged, along with Per Ullidtz, for his assistance in implanting the method, and testing within *CalME*.

REFERENCES

1. National Cooperative Highway Research Program (NCHRP). *Guide for mechanistic-empirical design of new and rehabilitated pavement structures*. National Cooperative Highway Research Program, Washington, DC, 2004.
2. Larson, G. and B. Dempsey. EICM Software. Enhanced Integrated Climatic Model (EICM) Version 3.0. Urbana, Illinois: University of Illinois, 2003.
3. Darter, M., L. Khazanovich, T. Yu and J. Mallela. *Reliability Analysis of Cracking and Faulting Prediction in the New Mechanistic-Empirical Pavement Design Procedure*. Transportation Research Record: Journal of the Transportation Research Board, No. 1936, 2005, pp. 150-160.
4. Ongel, A. and J.T. Harvey. *Analysis of 30 Years of Pavement Temperatures using the Enhanced Integrated Climate Model (EICM)*. Partnered Pavement Research Center, University of California, Berkeley and Davis, 2004.
5. Baltzer, S., H.J. Ertman-Larson, E.O. Lukanen and R.N. Stubstad. "Prediction of AC Mat Temperature for Routine Load/Deflection Measurements". Proceedings of the *4th International Conference on Bearing Capacity of Roads and Airfields, Volume 1*. Minneapolis, MN, 1994, pp. 401-412.
6. Harvey, J.T and J.D. Lea. March 21st, 2007. Email communication with M. Darter and L. Khazanovich.
7. Wang, D., J.R. Roesler and D.-Z. Guo. Analytical Approach to Predicting Temperature Fields in Multilayered Pavement Systems. ASCE Journal of Engineering Mechanics, Vol. 135, 2009, pp. 334-344.
8. Hughes, T.J.R. 2000. *The finite element method: linear static and dynamic finite element analysis.* Dover Publications.
9. United States Environmental Protection Agency (EPA). *Reducing Urban Heat Islands: Compendium of Strategies—Cool Pavements*. 2008.
10. Kaloush, K.E., J.D. Carlson, D. Joby, J.S. Golden and P.E. Phelan. *The Thermal and Radiative Characteristics of Concrete Pavements in Mitigating Urban Heat Island Effects*. Report SN2969, Portland Cement Association, Skokie, IL, 2008.
11. Xu, Q.W. and M. Solaimanian. *Modeling temperature distribution and thermal property of asphalt concrete for laboratory testing applications.* Construction and Building Materials, Vol. 24(4), 2010, pp. 487-497.
12. Mrawira, D. and J. Luca. *Effect of aggregate type, gradation, and compaction level on thermal properties of hot-mix asphalts.* Canadian Journal of Civil Engineering, Vol. 33(11), 2006. pp. 1410-1417.
13. Luca, J. and D. Mrawira. *New Measurement of Thermal Properties of Superpave Asphalt Concrete*. ASCE Journal of Materials in Civil Engineering, Vol. 17, 2005. pp. 72-79.

14. Côté, J. and J.-M. Konrad. *Thermal conductivity of base-course materials*. Canadian Geotechnical Journal, Vol. 42, 2005, pp. 61-78.
15. Côté, J. and J.-M. Konrad. *A generalized thermal conductivity model for soils and construction materials.* Canadian Geotechnical Journal, Vol. 42, 2005, pp. 443-458.
16. Côté, J. and J.-M. Konrad. *Estimating Thermal Conductivity of Pavement Granular Materials and Subgrade Soils.* Transportation Research Record: Journal of the Transportation Research Board, No. 1967, 2006, pp. 10-19.
17. Frankenstein, S. and G.G. Koenig. *Fast All-season Soil STrength (FASST)*. Cold Regions Research and Engineering Laboratory, Engineering Research and Development Center, US Army Corps of Engineers, 2004.